Safferling et al., http://www.jcb.org/cgi/content/full/jcb.201212020/DC1

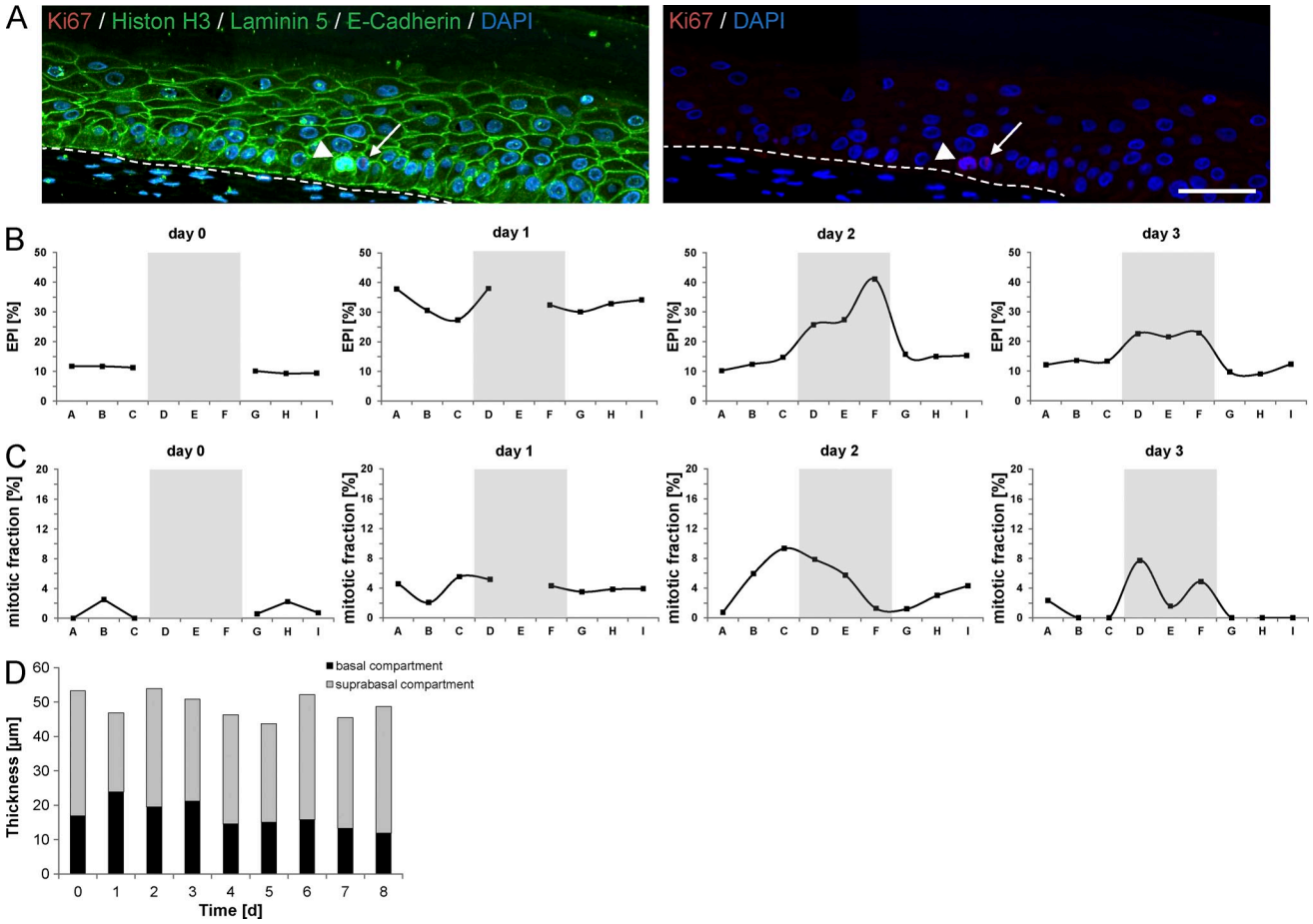

Figure S1. **Comparison of EPI to mitotic fraction and the effect on epidermal thickness.** (A) Double fluorescent staining of Ki67 and phospho-histone 3 (p-H3). Proliferating cells were Ki67$^+$ (white arrow), whereas mitotic events were Ki67$^+$/p-H3$^+$ double positive (white arrowhead). Broken lines denote the basal membrane. The wound cultures were separated into nine regions of identical size. (B and C) The EPI (B) and the mitotic index (C) were spatially and temporally evaluated by analyzing each region independently. The wound region is highlighted in gray. The data shown are from a single representative experiment out of two repeats; n = 3 (day 0 [d0]), 3 (day 1), 3 (day 2), and 3 (day 3); 48 slides were analyzed in total; data are means. (D) A systematic morphometric analysis of unwounded tissue regions during reepithelialization based on CK10, CK14 double staining was performed over a period of 8 d using image processing of histological sections. Epidermal thickness was measured on the basis of the expression pattern of these markers. n = 17 from a single experiment. Bar, 50 µm.

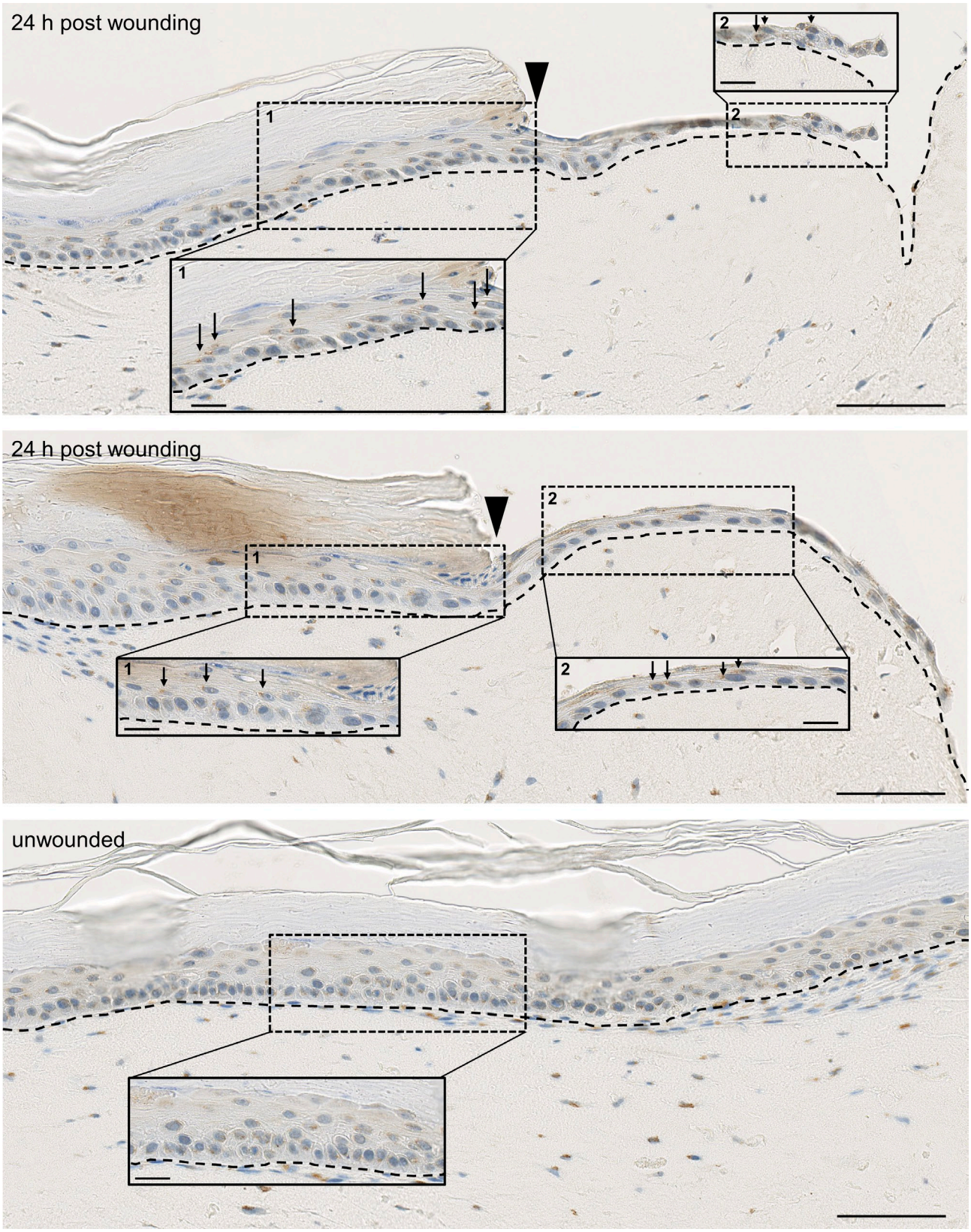

Figure S2. **Golgi positioning in polarized migrating cells.** Histological sections of representative wounded (24 h after wounding) and unwounded EETs showing a DAB-staining of golgin A2, indicating the Golgi complex. When cells had started to migrate, the Golgi complex translocated behind the nucleus in an opposed direction of migration (black arrows). In unwounded cultures, the Golgi complex showed a random orientation with a trend to be positioned underneath the nucleus. Magnifications of the regions of interest within the EET are shown in the insets. Arrowheads indicate the wound margin. Broken lines denote dermal–epidermal junction. Bars: (overview screens) 100 µm; (insets) 25 µm.

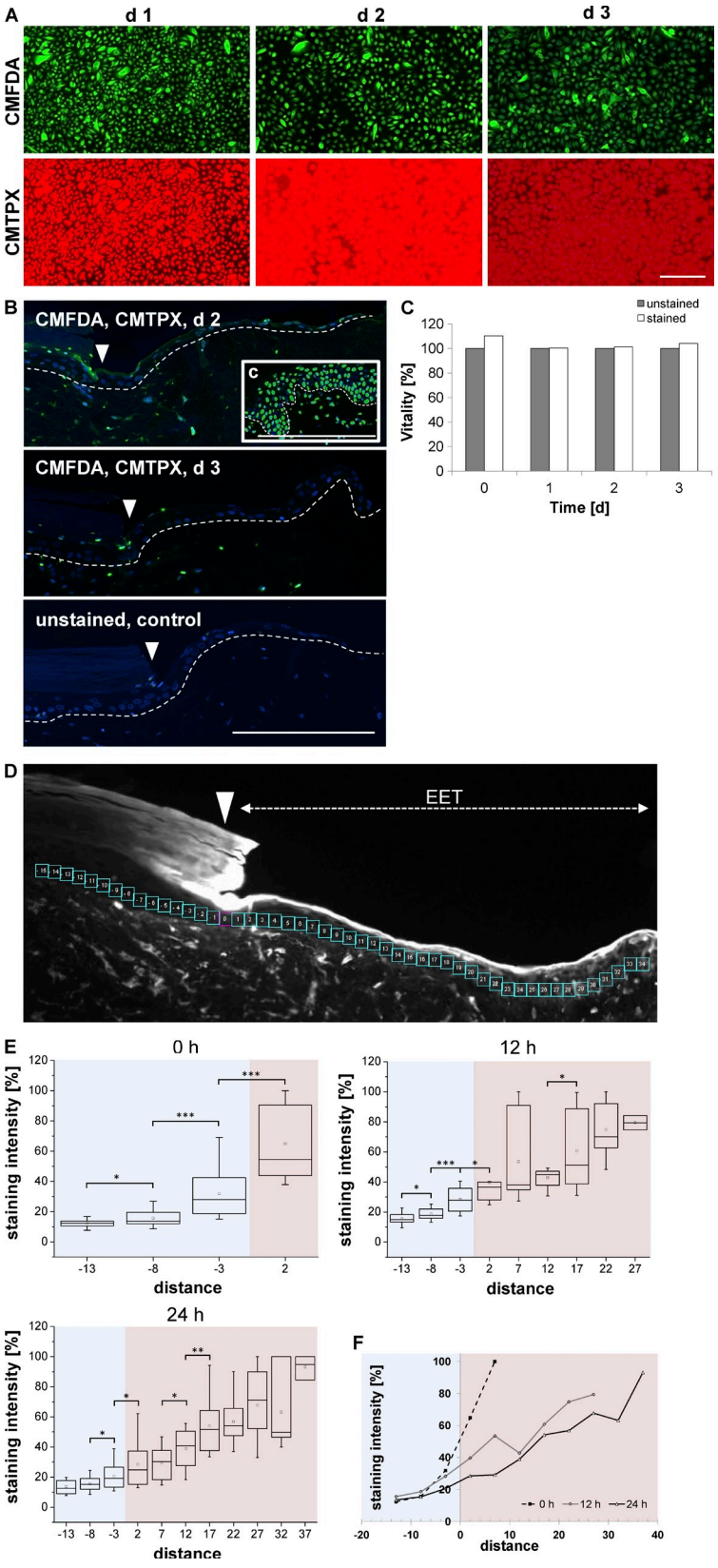

Figure S3. **Effect of the cell trackers CMFDA and CMTPX on primary human keratinocytes and organotypic wound cultures.** (A) 1-, 2-, and 3-d tracking of CMFDA/CMTPX double-stained primary human keratinocytes. (B) TUNEL assay of representative EETs 2 and 3 d after CMFDA/CMTPX staining and an unstained EET as a negative control. (inset) DNase-treated normal human epidermis was used as a positive control. (C) MTT test of CMFDA/CMTPX-stained and unstained wound cultures 0, 1, 2, and 3 d after staining. n = 6 (day 0 [d0]), 6 (day 1), 6 (day 2), and 6 (day 3) from a single experiment; data are means. (D) Continuous spatial analysis of fluorescent dye (CMTPX) in the EET, using computational image processing. The figure shows the EET, extending from the wound margin (left) into the wound bed (dashed line). Staining intensity in the basal layer is averaged over five subsequent small windows (cyan) and depicted as one data point in E and F. (E) Box plots for three time points (0, 12, and 24 h) of tracking CMTPX in wounded (red area) and unwounded (blue area) regions. Maximum CMTPX staining intensity was normalized to 100% for each EET. Boxes indicate the 25th and 75th percentile. Whisker denote the outliers. Dots indicate the mean, and horizontal lines indicate the median. n = 4 (0 h), 3 (12 h), and 4 (24 h) from a single experiment; *, $P \leq 0.05$; **, $P \leq 0.01$; ***, $P \leq 0.001$, Student's t test. (F) Comparison of the averaged values of the three time points. This experiment was completed once (n = 11). Arrowheads indicate the wound margin. Broken lines denote dermal–epidermal junction. Bars, 300 µm.

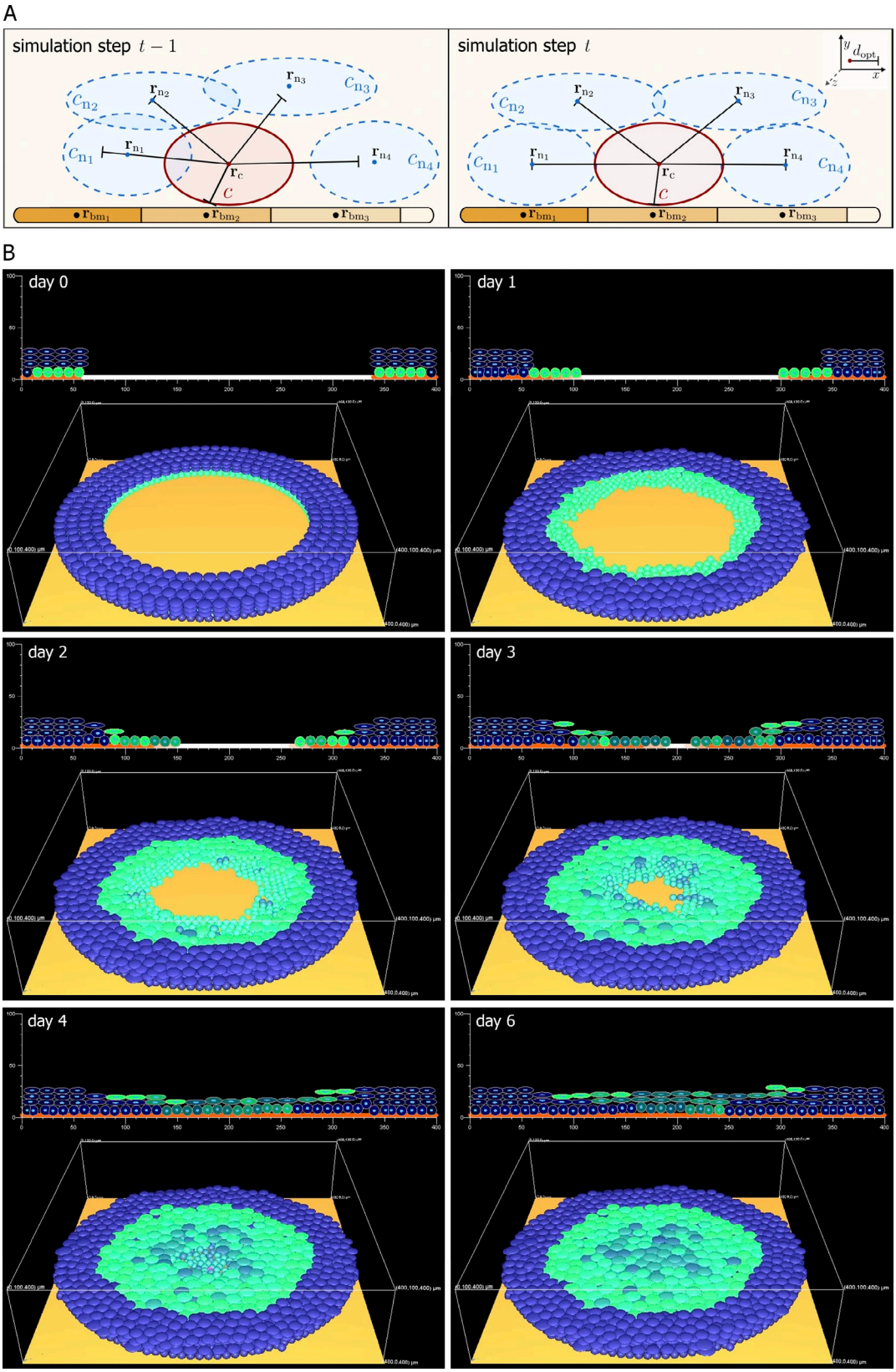

Figure S4. **In silico biomechanical cell model and 2D and 3D simulation of the ESM.** (A) In the center-based BM, a cell is represented by an ellipse (2D) or ellipsoid (3D). A cell's position in space is given by its center of mass r. The considered cell *c* (depicted in red) balances the distance to all neighboring cells and the basal membrane. In the case of optimal balancing from one simulation step $t-1$ to the following step *t*, the cell's center of mass r_c is in optimal distance d_{opt} to all neighboring cells' $\mathbf{r}_{n_i}$ and the center $\mathbf{r}_{bm_i}$ of the closest section *i* of the discretized basal membrane. The calculation of this balance involves intercellular pressure in the case of cell c_{n_1} or cell–cell adhesion in case of cells c_{n_3} and c_{n_4}. (B) Simulation of the 2D and the 3D ESM model. Between day 0 and 1, an EET develops. From day 1 to 3, a triangular structure composed of early suprabasal cells and basal cells emerges. Between day 3 and 4, the wound gap was completely (100%) reepithelialized. Day 6 shows a fully reepithelialized and stratified neo-epidermis.

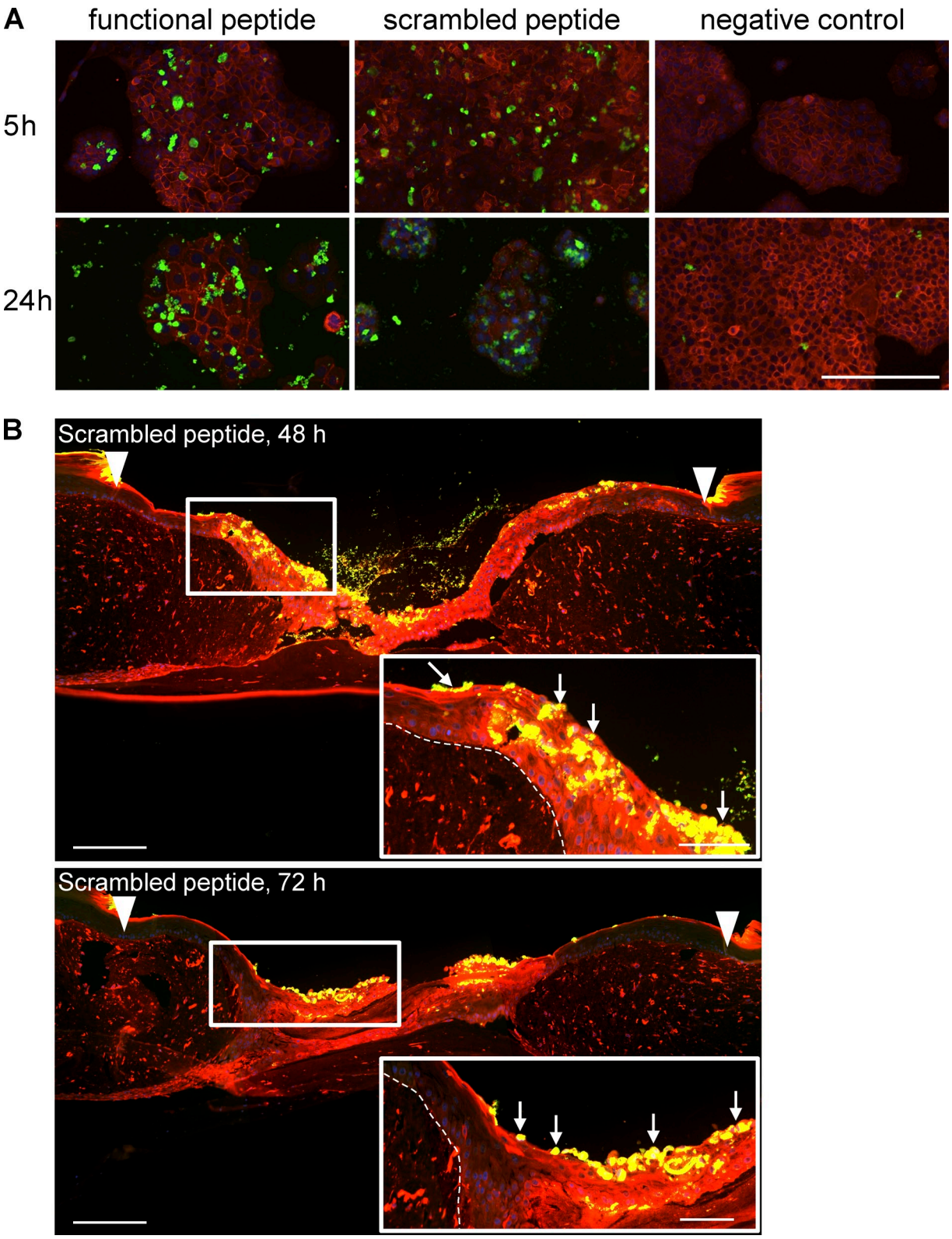

Figure S5. **Characterization of synthetic functional and scrambled peptides emulating occludin loop B.** (A) HaCaT cells were treated for 5 and 24 h by applying 200 µM functional or scrambled peptides. Peptide complexes accumulated at the tight junction protein occludin. Bar, 300 µm. (B) Organotypic cultures were wounded, and 400 µM scrambled peptide was applied within a 6-h period of time. Occludin-blocked cells (white arrows) concentrated in the suprabasal compartment and were shed with progressing time. Insets show magnified areas of the EET to illustrate the effect of the scrambled peptide. Arrowheads indicate the wound margin. Broken lines denote dermal–epidermal junction. Bars: (overview screens) 250 µm; (insets) 100 µm.

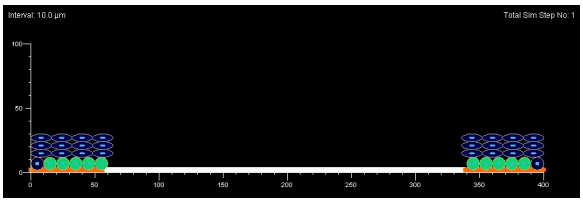

Video 1. **2D simulation of the ESM.** The video is showing the in silico CBM simulating the ESM in 2D. Images were taken by capturing the screen of the simulation window of the EPISIM platform for each simulation step.

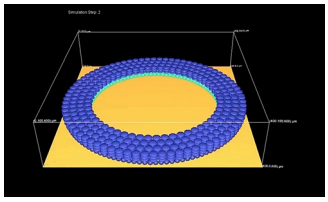

Video 2. **3D simulation of the ESM.** The video is showing the in silico CBM simulating the ESM in 3D. Images were taken by capturing the screen of the simulation window of the EPISIM platform for each simulation step.

A Word document is also provided online that includes the MATLAB source code of the major axis analysis.